Available online at www.sciencedirect.com
ScienceDirect
Acta Materialia xxx (2009) xxx–xxx
Acta MATERIALIA
www.elsevier.com/locate/actamat

Energy landscape for martensitic phase transformation in shape memory NiTi

S. Kibey [a], H. Sehitoglu [a,*], D.D. Johnson [b]

[a] Department of Mechanical Science and Engineering, University of Illinois, Urbana-Champaign, 1206 W. Green St., Urbana, IL 61801, USA
[b] Department of Material Science and Engineering, University of Illinois, Urbana-Champaign, 1304 W. Green St., Urbana, IL 61801, USA

Received 15 July 2008; received in revised form 26 November 2008; accepted 1 December 2008

Abstract

First-principles calculations are presented for parent B2 phase and martensitic B19 and B19′ phases in NiTi. The results indicate that both B19 and B19′ are energetically more stable than the parent B2 phase. By means of ab initio density functional theory, the complete distortion–shuffle energy landscape associated with B2 → B19 transformation in NiTi is then determined. In addition to accounting for the Bain-type deformation through the Cauchy–Born rule, the study explicitly accounts for the shuffle displacements experienced by the internal ions in NiTi. The energy landscape allows the energy barrier associated with the B2 → B19 transformation pathway to be identified. The results indicate that a barrier of 0.48 mRyd atom^{-1} (relative to the B2 phase) must be overcome to transform the parent B2 NiTi to orthorhombic B19 martensite.

Keywords: NiTi; Martensitic phase transformation; Shape memory alloys; Density functional theory; Nickel alloys

1. Introduction

Equiatomic NiTi has emerged as an important technological material owing to its shape memory behavior [1,2]. At high temperatures, NiTi exhibits a cubic B2 (CsCl) structure and undergoes a reversible B2 → B19′ martensitic transformation (MT) which gives rise to its shape memory effect [1]. At the atomic scale, this transformation involves distortions and shuffles (finite local displacements) of the internal atoms. However, the energy pathway associated with this distortion–shuffle transformation in NiTi is not clear. Here, ab initio density functional theory calculations are presented to determine the energy landscape associated with the B2 → B19 transformation in NiTi, as well as the correct distorted B19′ phase. It is shown that a finite barrier exists between the parent B2 and the product martenstic phase which governs the reversibility of the transformation. The energy barrier associated with the unstable configuration or transition state (TS) is calculated. An external driving force such as stress or temperature is needed to overcome this energy barrier. Ultimately, the ideas presented here will pave the way for the design of new shape memory alloys.

2. Martensitic transformation in NiTi

Although, the MT in equiatomic NiTi is well known, the mechanism for the transformation is not well understood. Owing to experimental difficulties in directly observing the MT pathways, the microscopic mechanisms and the associated pathways for some well-known transformations (e.g. Bain transformation) have been proposed based purely on the orientation relationships between the parent and the product martensite phases [3–6]. No formal mechanism has yet been proposed for the MT in NiTi [7–10]. Ackland et al. [9] reported the energies of parent B2 and product B19′ structure, and an additional metastable bco phase. However, their study did not address the issue of

* Corresponding author. Tel.: +1 217 333 4112; fax: +1 217 244 6534.
E-mail addresses: huseyin@illinois.edu, huseyin@uiuc.edu (H. Sehitoglu).

1359-6454/$34.00 © 2008 Acta Materialia Inc. Published by Elsevier Ltd. All rights reserved.
doi:10.1016/j.actamat.2008.12.008

determining the energy landscape associated with the MT in NiTi. Zhang and Guo [10] computed the energy landscape for B2–B19 transformation, but their work does not explicitly address the role of simultaneous distortion and shuffle of the lattice during MT in NiTi. Further, it is not clear from their study how the NiTi transformation pathway energies vary with shuffles. The present paper addresses the above issue.

Determining the energy landscape and, thereby, the actual energetically favorable pathway for NiTi is important, because the associated energy barriers affect the reversibility of the transformation. This paper addresses the determination of the transformation pathway, and specifically the change in energy to surmount the energy barrier for transformation. The determination of the transformation pathway associated with MT in NiTi is addressed using ab initio density functional theory, and a systematic mathematical formulation is presented to account explicitly for the role of in-plane shuffles and volumetric distortion of the NiTi lattice on its energy landscape.

Fig. 1 shows the three primary phases involved in MT of NiTi (adapted from Ref. [9]). For clarity, the (1 1 0) projections of each of three phases are also shown in Fig. 1a–c. Parent NiTi lattice is a cubic B2 phase (CsCl-type structure) with a lattice constant [8] of $a_{B2} = 0.3015$ nm (see Fig. 1a). The B19 phase shown in Fig. 1b is an orthorhombic phase. Relative to the parent body-centered tetragonal (bct) phase, the B19 phase involves a volumetric distortion and a local shuffle of the interior Ni and Ti atoms along the $[0\,1\,0]_{B19}$ direction. Fig. 1c shows the B19′ phase, which is a slight monoclinic distortion of the orthorhombic phase. It is seen that the orthorhombic B19 phase and the monoclinic B19′ phase differ in the monoclinic distortion of angle β from 90° to 97.78°. First, the equilibrium structures and stable energies of these three phases in NiTi are determined, and then the pathways involved are investigated.

3. Equilibrium structures of NiTi phases

Here, the lattice parameters and the atomic positions of B2, B19 and B19′ phases in NiTi are computed using the Vienna ab initio Simulation Package [11,12] (VASP) and the generalized gradient approximation [13] (GGA) is implemented on a projector augmented wave [14] (PAW) basis. Each unit cell consisted of four atoms. For all NiTi structures, Brillouin zone sampling was performed using 16×16×16 special k-point mesh [15] with 302.0 eV energy cutoff, ensuring convergence of energy within 1 meV atom^{-1}. Volume relaxations were allowed for all three lattices, and ionic relaxations were permitted for all the ions in each lattice. Table 1 summarizes the computed lattice parameters. The results are compared with the experimental data (note that no experimental data are available for orthorhombic B19 NiTi) and other first-principles calculations. The computed lattice constants vary slightly with different DFT implementations (for example, LDA vs. GGA, FLAPW vs. USPP or PAW), but are in good agreement with each other and with the experimental data. In addition, the calculations of lattice parameters in Table 1

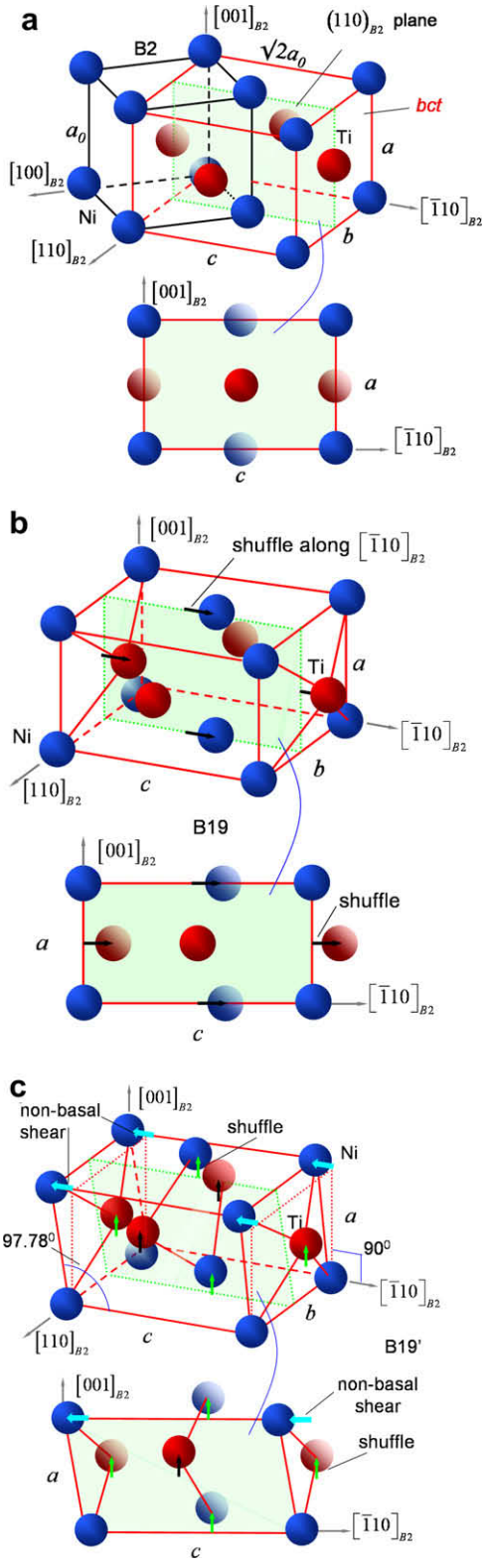

Fig. 1. Lattice structures in NiTi: (a) B2 cubic lattice and the ideal bct lattice; (b) orthorhombic B19 martensite with the allowed shear and shuffle; (c) monoclinic B19′ martensite with shear and shuffle.

Table 1
VASP–PAW–GGA calculated structural parameters a, b and c (in Å) for B2, B19 and B19′ phases in NiTi, compared with experimental data and other ab initio studies. The computed lattice parameters for all three structures are in good agreement with the experimental data of Kudoh et al. [7] and other first-principles studies.

	B2			B19			B19′			
	Present calc.	Exp.†	Other calc.‡	Present calc.	Other calc.		Present calc.	Exp.*	Other calc.	
a	3.011	3.015	3.009	2.8098	2.776‡	2.73§	2.847	2.898	2.929‡	2.88§
b	4.2583	4.2639	4.2554	4.1890	4.221‡	4.07§	4.1162	4.108	4.048‡	4.12§
c	4.2583	4.2639	4.2554	4.7074	4.631‡	4.64§	4.6724	4.646	4.686‡	4.62§

† Ref. [8].
‡ VASP–USPP–GGA [9].
§ FLAPW–LDA [10].
* KTMO [7].

indicate that B19 and B19′ martensitic lattice structures are very close to each other, except for the monoclinic distortion from 90° to $\beta = 97.78°$ (see Fig. 1). This angle was calculated in the present study by relaxing of the initial structure, and is in agreement with experiments.

The stable energies of these phases were computed, corresponding to the determined lattice parameters given in Table 1. Table 2 compares the energies relative to B2 for all three structures in NiTi. Calculations indicate that the B19 phase is lower in energy than the B2 phase by 2.1 mRyd atom^{-1} and hence is energetically more stable than the parent B2 phase. Note that the present results for the lattice constants compare well with the calculations of Ackland et a1. [9] and Ye et a1. [16], but the energies predicted by Zhang and Guo [10] differ significantly from the rest of the studies. However, note that Ackland's work suggests the presence of a new phase BCO (body-centered orthogonal). To the authors' knowledge, no experimental or theoretical studies have proposed the presence of a BCO phase in NiTi martensites. The theoretical results confirm that the monoclinic structure B19′ is the NiTi martensitic phase with the lowest energy. The calculations also indicate that the observed monoclinic B19′ phase is the lowest in energy ($E_{B19'} - E_{B2} = -2.9$ mRyd atom^{-1}). This suggests that the B19′ phase may be considered the ground state for all NiTi-based alloys. It is also seen that B19 and B19′ phases are energetically close to each other. This is expected, as the results in Table 1 reveal that the two phases are structurally close to each other.

Table 2
VASP–PAW–GGA computed energies E–E_{B2} (in mRyd atom^{-1}) for B2, B19 and B19′ phases in binary NiTi. All energies are relative to parent the B2 phase considered the reference state. Present results are also compared with other ab initio calculations: HAR denotes Ackland et al. [9]; ZG denotes Zhang and Guo [10]; YCH denotes Ye et al. [16].

Structure	$E - E_{B2}$			
	Present calc.	HAR†	ZG‡	YCH*
B2	0	0	0	0
B19	−2.1	−2.21	−1.4	−2.05
B19′	−2.9	−3.08	−1.7	−3.45

† VASP–USPP–GGA [9].
‡ FLAPW–LDA [10].
* PP–LDA [16].

4. Ab initio determination of transformation pathway

Clearly, the pathway for direct B2 → B19′ transformation in NiTi requires non-trivial addressing of the (i) lattice distortion, (ii) non-basal lattice shear, as well as the (iii) in-plane and out-of-plane shuffles. However, B2 → B19 transformation involves (i) lattice distortion and (ii) in-plane shuffles, thus, reducing the number of independent degrees of freedom. Also, as noted in Table 2, the B19 NiTi phase lies energetically between the B2 and B19′ structures. Hence, the orthorhombic B19 phase can be expected to be an intermediate configuration during direct B2 → B19′ transformation in binary NiTi. The possibility of this pathway was postulated by Hehemann and Sandrock [17] but, unlike the present results, no quantitative arguments were offered. Ye et al. [16] proposed a B2–B19′ transformation pathway using a linear interpolation of the atomic positions between the B2 and B19′ phases. However, as seen above, the B2–B19′ transformation involves complex distortions and shuffles which cannot be captured through interpolation. Here, a rigorous approach is presented to account for the effect of distortions and shuffles on the NiTi energy landscape. Based on the present lattice structure and stable energy calculations, it appears that determining the B2 → B19 pathway for equiatomic NiTi is likely to provide significant insight into the B2 → B19′ transformation. As a first step towards determining the B2 → B19 → B19′ pathway for complete transformation, the study focuses on the B2 → B19 pathway.

Fig. 2 shows a schematic of the parent bct NiTi phase and the orthorhombic B19 martensite. Also shown are the $\{110\}_{B2}$ projections (equivalent to $\{100\}_{B19}$ projections) of two lattices to illustrate clearly the cell deformations and shuffles involved in the transformation. During the B2 (bct) → B19 transformation, the interior (non-Bravais lattice points) Ni and Ti atoms in the orthorhombic B19 phase undergo a normalized shuffle of approximately $\frac{1}{8}[010]_{B19}$ [17]. Other ab initio studies [10] calculated the magnitude of this normalized shuffle as 0.098 along $[010]_{B19}$. Conceptually, the orthorhombic distortion and the shuffle can be viewed as sequential "steps" in the B2 → B19 transformation [17] but, physically, both shuffle and orthorhombic distortion most likely occur simulta-

Please cite this article in press as: Kibey S et al., Energy landscape for martensitic phase transformation ..., Acta Mater (2009), doi:10.1016/j.actamat.2008.12.008

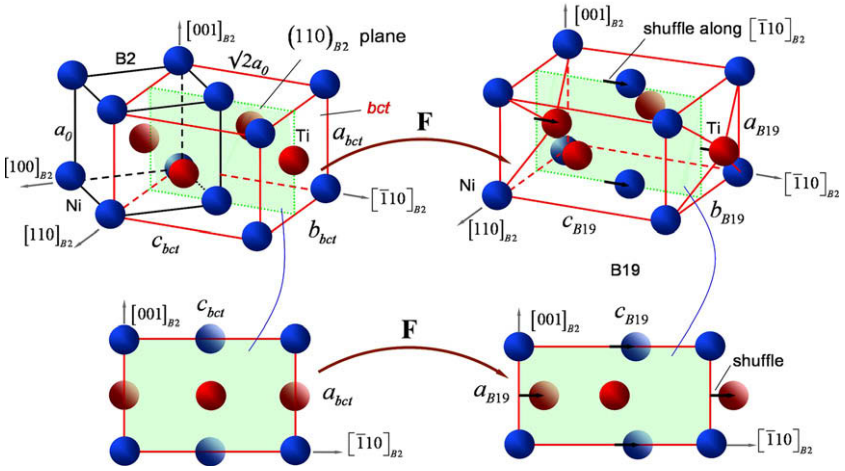

Fig. 2. Schematic of B2 (bct) → B19 transformation in NiTi. Also shown are the $\{110\}_{B2}$ projections (equivalent to $\{100\}_{B19}$ projections) of two lattices to illustrate clearly the cell deformations and shuffles involved in the transformation.

neously. The ab initio calculations have explicitly accounted for the concurrent distortion and shuffles.

In order to determine the transformation (energy) pathway for B2 → B19 transformation, the crystal distortions and shuffles at the atomic scale need to be correlated with the continuum displacements at the macro scale. This is achieved through the Cauchy–Born (CB) rule [18–20], which relates the changes in the atomic positions to the macroscopic displacements through a local deformation gradient **F**. For a simple lattice deforming to another simple lattice, the CB hypothesis implies a homogeneous deformation in which the basis vectors in the deformed simple lattice can be related to the basis vectors of the parent lattice as follows:

$$a_m = \mathbf{F} a_i \tag{1}$$

where the basis vectors a_i and a_m belong to the parent and the martensite lattices, respectively. The CB rule given by Eq. (1) assumes that atomic positions change in a continuous manner with pressure and temperature. However, B2 → B19 transformation involves abrupt shuffles, which lead to discontinuity in **F**. To account for the discontinuity due to shuffles, the CB rule was implemented as follows: the parent bct structure is substituted by the Bravais lattice, and the CB rule is imposed on the Bravais lattice vectors alone. This implies that the atoms at the Bravais sites in the parent lattice change position according to the CB rule. To account for the internal displacements associated with the shuffles, the strain energy density W is minimized with respect to the shuffle displacements as the applied deformation gradient **F** is held fixed [20]. This minimization can be achieved by relaxing the internal ions to the local energy minimum without allowing for volume change (fixed **F**). After minimization, the equilibrium shuffle displacements can be determined. Thus, the strain energy density will now be a function of imposed deformation **F** only. Note that internal relaxations may not be negligible even for very small imposed strains (as is the case for B2 NiTi). Hence, appropriate internal relaxations are essential to determine the correct structural energies of the intermediate configurations.

The basis vectors of the parent bct NiTi lattice are

$$e_1^{\mathrm{bct}} = a_0 \begin{pmatrix} 1 \\ -1 \\ 0 \end{pmatrix};\ e_2^{\mathrm{bct}} = a_0 \begin{pmatrix} 1 \\ 1 \\ 0 \end{pmatrix};\ e_3^{\mathrm{bct}} = a_o \begin{pmatrix} 0 \\ 0 \\ 1 \end{pmatrix} \tag{2}$$

whereas for the orthorombicB19 martensite they are

$$e_1^{\mathrm{B19}} = \frac{b}{\sqrt{2}} \begin{pmatrix} 1 \\ -1 \\ 0 \end{pmatrix};\ e_2^{\mathrm{B19}} = \frac{c}{\sqrt{2}} \begin{pmatrix} 1 \\ 1 \\ 0 \end{pmatrix};\ e_3^{\mathrm{B19}} = a \begin{pmatrix} 0 \\ 0 \\ 1 \end{pmatrix} \tag{3}$$

Using the CB rule, the B2 → B19 deformation can be described as

$$e_i^{\mathrm{B19}} = \mathbf{F} e_i^{\mathrm{bct}} \tag{4}$$

$$\mathbf{F} = \begin{bmatrix} b/a_0\sqrt{2} & b/a_0\sqrt{2} & 0 \\ c/a_0\sqrt{2} & c/a_0\sqrt{2} & 0 \\ 0 & 0 & a/a_0 \end{bmatrix} \tag{5}$$

It is now assumed that the lattice parameters a_i, b_i and c_i vary linearly at any intermediate state i during the B2 → B19 transformation, and they are expressed in the following parametric form:

$$b_i(\lambda) = a_0\sqrt{2} + \lambda(b - a_0\sqrt{2}) \tag{6}$$

$$c_i(\lambda) = a_0\sqrt{2} + \lambda(c - a_0\sqrt{2}) \tag{7}$$

$$a_i(\lambda) = a_0\sqrt{2} + \lambda(a - a_0) \tag{8}$$

with B2($\lambda = 0$) and B19($\lambda = 1$) structures as the end states. The deformation gradient can then be written as follows:

$$\mathbf{F} = \begin{bmatrix} b_i(\lambda)/a_0\sqrt{2} & b_i(\lambda)/a_0\sqrt{2} & 0 \\ c_i(\lambda)/a_0\sqrt{2} & c_i(\lambda)/a_0\sqrt{2} & 0 \\ 0 & 0 & a_i(\lambda)/a_0 \end{bmatrix} \tag{9}$$

Please cite this article in press as: Kibey S et al., Energy landscape for martensitic phase transformation ..., Acta Mater (2009), doi:10.1016/j.actamat.2008.12.008

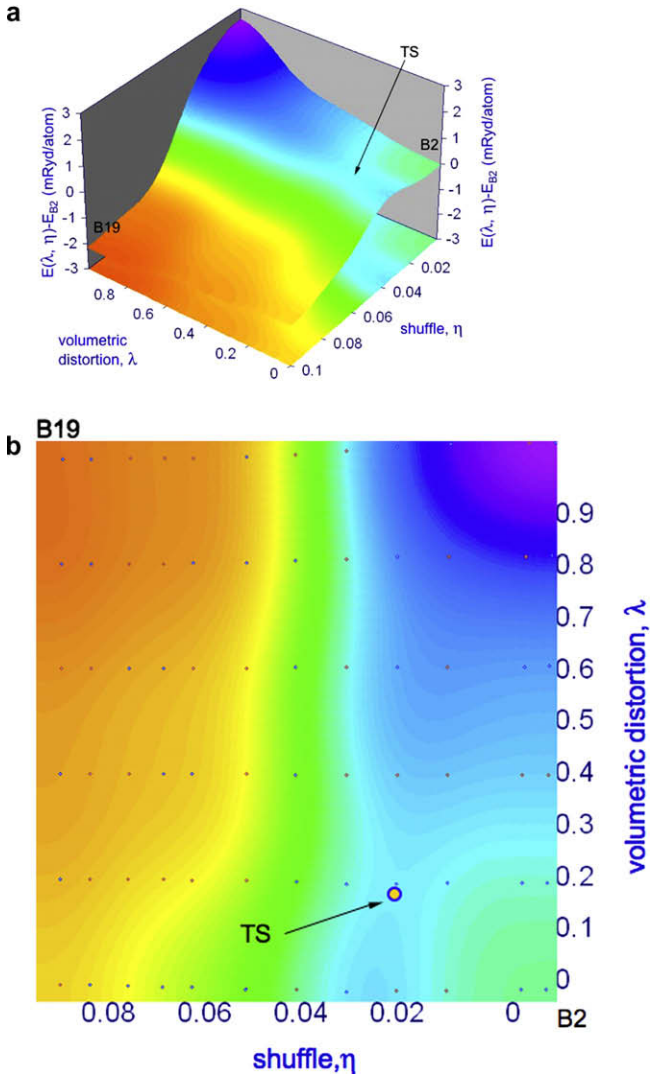

Fig. 3. (a) Energy landscape (in mRyd atom^{-1}) for B2–B19 transformation in equiatomic NiTi as a function of distortion parameter λ and shuffle η. The energy difference $E_{B19} - E_{B2}$ is -2.1 mRyd atom^{-1}. It is seen that a finite barrier (transition state, denoted by TS) exists between the B2 and B19 phases. (b) Contour plot of the energy landscape shown in (a). The MEP will involve minimum distortion and shuffle. The point at which highest energy is encountered is identified as TS and is located at point $\lambda,\eta = (0.2, 0.035)$ (indicated by the arrow). The magnitude of the energy barrier is 0.48 mRyd atom^{-1} (relative to the parent B2 phase).

The internal ions undergo a shuffle (see Fig. 2) which must be accounted for separately. Previous first-principles calculations [10] predicted a normalized shuffle of 0.098 in the $[0\,1\,0]_{B19}$ direction (see Fig. 2), while Hehemann and Sandrock [17] predicted the normalized magnitude as 0.125 for the B19′ phase, which is close to the shuffle in the B19 phase. The above deformation gradient $\mathbf{F}(\lambda)$ maps the Bravais points only, but does not include the shuffles. To account for the associated shuffle displacements of the interior atoms, equal initial shuffles were superimposed on all interior atoms in addition to the deformation $\mathbf{F}(\lambda)$. The shuffles were defined by the normalized shuffle parameter $\eta = s/c$, where s is the absolute shuffle. The strain energy density W was then minimized with respect to η at fixed $\mathbf{F}$. This minimization was achieved by relaxing the internal ions to the local energy minimum without allowing for volume change (fixed $\mathbf{F}$), resulting in the final stable shuffle positions of the internal ions. The actual transformation pathway was determined as a function of the distortion parameter λ and η. The *entire* energy landscape for B2 → B19 transformation was computed by varying the deformation gradient from $\lambda = 0$ to 1 for a fixed value of shuffle η. For B19 NiTi, the landscape was completed by exploring all possible combinations (λ,η) and, while η was varied from 0 to 0.125. The actual shuffle at minimum energy was found to change from the initial imposed shuffle of 0.125 to an equilibrium shuffle of 0.098 after internal relaxation.

5. Results and discussion

No energy pathways incorporating distortion and shuffle are given in previous studies, and this is the first time the energy landscape for NiTi phase transformation has been clearly described. Fig. 3a shows the energy landscape for the B2–B19 transformation in binary NiTi as a function of distortion λ and shuffle η. Note that $\lambda,\eta = (0,0)$ corresponds to the initial B2 phase, while $\lambda,\eta = (1, 0.098)$ corresponds to the final B19 phase with an energy difference $E_{B19} - E_{B2}$ of -2.1 mRyd atom^{-1}, indicating that the B19 phase is energetically more stable than the B2 phase, as also noted in Table 2. From Fig. 3a, it is seen that a finite barrier exists between the B2 and B19 phases which depends on the transformation path followed by the alloy. Fig. 3b shows the contour plot of the energy landscape. In principle, the specific trajectory followed by NiTi during the transformation will involve a minimum energy barrier (which is likely to be the TS depicted here) and also minimum distortion and shuffle. Note that the exact minimum energy path (MEP) for this transformation must be determined from numerical optimization [21–26]. Note that the direction of steepest gradient starting from parent B2 phase involves a maximum energy barrier (denoted by TS) of 0.48 mRyd atom^{-1} at $\lambda,\eta = (0.2, 0.035)$ relative to the parent B2 phase. The energy barrier must be overcome to transform the parent B2 into the orthorhombic B19 phase. As a comparison, Zhang and Guo [10] predicted a barrier of 0.40 mRyd atom^{-1} from the B2 side between the two phases. From Fig. 3a, it is found that the steepest gradient path in the neighborhood of B2 NiTi involves almost equal amounts of shuffle and distortion. However, after a normalized shuffle $s = 0.01$ is reached, shuffle will dominate volumetric distortion until the barrier at $\lambda,\eta = (0.2, 0.035)$ is overcome. Beyond the transition point TS, the transformation pathway will be downhill, and lattice will preferentially undergo volumetric distortion that will dominate shuffle.

The determination of energy landscape and the transition barrier for NiTi MT is essential for determining the transformation stress. Recently, it was shown that the

Please cite this article in press as: Kibey S et al., Energy landscape for martensitic phase transformation ..., Acta Mater (2009), doi:10.1016/j.actamat.2008.12.008

stress required for activation of twinning in fcc materials is controlled by the energy barrier involved [27]. As MT is a more general deformation mode, it is expected that the activation stress for MT will depend on the energy barrier and also the energy landscape. The present calculations constitute important steps towards a more complete understanding of the shape memory effect. Note that the overall B2 → B19′ energy landscape could be relatively complex and needs to be determined to establish the driving forces for the transformation. Reversibility is favored when the energy landscapes for forward and reverse transformations involve paths with small and comparable unstable energy barriers. Specifically, a small energy differential between the initial state and the TS for the forward and reverse transformations would result in a small hysteresis. The phenomenological models for phase transformations ignore the entire energy pathway for the transformation, and thus are limited in assessing the hysteresis.

6. Conclusions

In summary, first-principles calculations were presented for parent B2 and martensitic B19 and B19′ phases in NiTi, which indicate that both B19 and B19′ are energetically more stable than the parent B2 phase, and B19′ is the lowest-energy state with the correctly predicted distortion angle. By means of ab initio density functional theory, the complete distortion–shuffle energy landscape associated with B2 → B19 transformation in NiTi was then determined. In addition to accounting for the Bain-type deformation through the CB rule, the shuffle displacements experienced by the internal ions in NiTi were explicitly accounted for. The energy landscape allows the identification of the asymmetric energy barrier (of 0.48 mRyd atom^{-1} relative to B2 phase) associated with the B2 → B19 transformation pathway, also responsible for the observed hysteresis upon reverse transformation, which will have to be overcome to transform the parent B2 NiTi to orthorhombic B19 martensite.

Acknowledgments

The authors acknowledge support from the National Science Foundation mainly under the Metals Program, DMR-03-13489 and DMR 08-03270, and partially from DMR-07-0089 and DMR-03-25939.

References

[1] Otsuka K, Wayman C, editors. Shape memory materials. Cambridge: Cambridge University Press; 1998.
[2] Bhattacharya K. Microstructure of martensite. New York: Oxford University Press; 2003.
[3] Bain E. Trans AIME 1924;70:25–46.
[4] Burgers W. Physica 1934;1:561–86.
[5] Silcock J. Acta Metall 1958;6(7):481–93.
[6] Bogers A, Burgers W. Acta Metall 1964;12:255–63.
[7] Kudoh Y, Tokonami M, Miyazaki S, Otsuka K. Acta Metall 1985;33(11):2049–56.
[8] Philip T, Beck PA. Trans AIME 1957;209:1269–71.
[9] Huang X, Ackland GJ, Rabe KM. Nat Mater 2003;2(5):307–11.
[10] Zhang JM, Gno GY. Phys Rev Lett 1997;78(25):4789–92.
[11] Kresse G, Hafner J. Phys Rev B 1993;47:558–61.
[12] Kresse G, Furthmuller J. Phys Rev 1996;B 54:11169–86.
[13] Perdew J, Wang Y. Phys Rev 1992;B 45:13244–9.
[14] Kresse G, Joubert D. Phys Rev 1999;B 59(3).
[15] Monkhorst HJ, Pack JD. Phys Rev B 1976;13:5188.
[16] Ye YY, Chan CT, Ho KM. Phys Rev B 1997;56:3678–89.
[17] Hehemann RF, Sandrock GD. Scripta Metall 1971;5(9):801–5.
[18] Ericksen JL. In: Gurtin M, editor. Phase tranformations and material instabilities in solids. Mathematics Research Center, University of Wisconsin New York: Academic Press; 1984. p. 61–77.
[19] Tadmor EB, Phillips R, Ortiz M. Philos Mag A 1996;73:1529–63.
[20] Tadmor EB, Smith GS, Bernstein N, Kaxiras E. Phys Rev B 1999;59(1):235–45.
[21] Gonzales C. J Chem Phys 1989;90:2154–60.
[22] Henkelman G, Uberuaga D, Jónsson H. J Chem Phys 2000;113:9901–4.
[23] Henkelman G, Jónsson H. J Chem Phys 2000;113:9978–85.
[24] Trinkle DR, Hennig RG, Srinivasan SG, Hatch DM, Jones MD, Stokes HT, et al. Phys Rev Lett 2003;91(2):025701.
[25] Caspersen KJ, Carter EA. Proc Natl Acad Sci USA 2005;102(19):6738–43.
[26] Burger S, Yang W. J Chem Phys 2006;124:054109–13.
[27] Kibey S, Liu I-B, Johnson D, Sehitoglu H. Acta Mater 2007;55:6843–51.

Please cite this article in press as: Kibey S et al., Energy landscape for martensitic phase transformation ..., Acta Mater (2009), doi:10.1016/j.actamat.2008.12.008